

Synthesis and Characterization of uniform Fine particles of Manganese Oxide and its Morphological Stability towards Calcination Rates

Khalida Akhtar*, Syed Sajjad Ali Shah, Muhammad Gul, Ikram Ul Haq and Naila Zubair
*National Center of Excellence in Physical Chemistry, University of Peshawar,
Peshawar-25120, Khyber Pukhtoonkhwa, Pakistan.*
khalida_akhtar@yahoo.com*

(Received on 15th February 2017, accepted in revised form 26th September 2017)

Summary: Fine particles of manganese oxide were synthesized by following the controlled precipitation method. For this, an aqueous solution of manganese chloride ($0.01\text{--}0.06\text{ molL}^{-1}$) were allowed to react with an aqueous solution of ammonium carbonate ($0.01\text{--}0.03\text{ molL}^{-1}$) at various temperatures ($25\text{--}60\text{ }^{\circ}\text{C}$) for different periods of time (10–40 min) with and without agitation (magnetic stirring/sonication). It was observed that the applied experimental parameters significantly affected different properties of the obtained solids. Extensive optimization of experimental parameters led to produce powders, composed of particles of uniform morphological features. The targeted particles were achieved only under limited experimental conditions. Selected batches were calcined at the elevated temperature ($800\text{ }^{\circ}\text{C}$) with the controlled heating rate of 5, 10 and $15^{\circ}\text{C}/\text{min}$. Scanning electron microscopic analysis and X-ray diffractometry of the calcined materials showed that neither the heating rate nor the final temperature affected the original morphology of the particles. Moreover, the same batches of the solids were also characterized by FTIR, XRD, and TG/DTA. It was found that the as synthesized particles were highly alike in morphology but were weakly crystalline in nature. However, heat treatment of the obtained particles resulted in Mn_2O_3 particles of orthorhombic crystal system of high crystallinity.

Keywords: Monodispersed; Controlled precipitation; Uniform particles; Manganese oxide.

Introduction

Regarding nano synthesis and nanofabrication, synthesis of fine particles in a controlled manner is the ultimate goal to achieve in the field of nanoscience and nanotechnology. Along with the chemical nature and composition, properties of the nanoparticles have also been found to be a function of their size, structure, shape, phase, and monodispersity [1]. Keeping in view the properties of uniform particles, researchers all around the world have been successful in the development of nanomaterials with diverse morphologies including nanospheres, nanowires, nanofibers, nanotubes, and nanobelts, etc. [2].

Oxide powders, comprising of nanosized particles are gaining the interest of the researchers across the globe, due to their importance in powder-based industries because of cost-effective processing, efficiency, better performance, and durability, etc. Oxides of transition metals are gaining importance for their wide range applications. Among the mentioned class of oxides, manganese oxide is an eminent member. Due to their extensive usage in a number of industries like batteries, adsorption, and catalysis, sensors, electrical and magnetic devices [3–5], synthesis of manganese compounds is being carried out on a large scale. Among various oxides of manganese, diamanganese trioxide (Manganese II oxide), is of high interest for its greater potential in

many fields including catalysis. Mn_2O_3 plays a key role in decomposition of nitrogen oxide & oxidation of compounds like carbon monoxide etc. [6] and it is best fit for fabrication of Li—Mn—O oxide cathode material for batteries [7]. Mn_2O_3 also finds its place in the fabrication of semiconducting gas sensors for detecting gases of environmental concern [8]. Keeping in view the extensive usage of the Mn_2O_3 , material scientists have tried to synthesize them by a number of ways. So far, they have been successful in obtaining them by different methods, including the low temperature reduction, microwave reflux method, microemulsion, hydrothermal, solid state reaction, redox reaction, electrochemical method and homogeneous precipitation, [9–11], etc.

In the recent years, development of simple ways and means to obtain precursors of Mn_2O_3 (MnCO_3) with different morphological features has received great importance. Scientists have been successful in obtaining nanosized MnCO_3 with different shapes and structures by following different techniques [12–14].

In this study, an attempt has been made to develop uniform fine particles of the precursor (MnCO_3) of nanosized Mn_2O_3 particles through controlled precipitation mechanism, after extensive optimization of several experimental parameters.

*To whom all correspondence should be addressed.

Then heat treatment at high temperatures transformed the as prepared MnCO_3 particles to nanosized Mn_2O_3 particles. The present study also reported the effect of high calcinations rates on the crystallinity and morphological features of the test material.

Experimental

Materials

A. R. grade manganese (II) chloride dihydrate (Merck), ammonium carbonate (Scharlau), ethanol (Scharlau), sodium nitrate (Scharlau), HCl (Merck), NaOH (Merck), KBr (Merck), were used as received. All the working and stock solutions were made in de-ionized water using Pyrex glass vessels.

Synthesis of Manganese Oxide Precursors (MnCO_3)

Manganese oxide precursor particles were prepared by using controlled precipitation route, where manganese chloride and ammonium carbonate were employed as the starting reagents. For this purpose, equal volumes of manganese chloride ($0.01\text{--}0.06\text{ molL}^{-1}$) and ammonium carbonate ($0.01\text{--}0.03\text{ molL}^{-1}$) solutions were mixed in a 250 mL reaction vessel at room temperature under mechanical agitation or silent conditions and aged for various intervals of time (10–40 min). The resulting precipitates were then isolated from the aqueous medium through membrane filters by vacuum filtration and washed extensively with deionized water and ethanol. The obtained powders were dried in air at room temperature and stored in a desiccator for further use.

Synthesis of manganese oxide (Mn_2O_3) nanoparticles

Heat treatment of the synthesized manganese oxide precursor powder was carried out in a Nabertherm, M7/11 furnace, equipped with the programmable controller. For this treatment, the selected samples were heated in the temperature range of $30\text{--}800\text{ }^\circ\text{C}$ at a controlled heating rate of 5°C , $10\text{ }^\circ\text{C}$ and $15\text{ }^\circ\text{C min}^{-1}$. After making the necessary setting in the furnace, each sample was heated to the final temperature of $800\text{ }^\circ\text{C}$ and then held for one hour at this temperature. The furnace was then turned off, and the sample was allowed to cool to room temperature inside the furnace. The heat-treated powder was stored in a desiccator to avoid absorption of moisture from environment on the powder surface.

Characterization

Scanning Electron Microscopy (SEM)

The morphological features and microstructure of the as synthesized and heat treated products were assessed by Scanning Electron Microscope (SEM: JSM-6490, JEOL). For carrying out SEM imaging, the desired powder samples were mounted on aluminum stubs with the help of conducting carbon tap and then sputtered with gold in an Auto Fine Coater (JFC-1600, JEOL) for a time interval of the 30s. The gold coated samples were then placed in the sample examination chamber of the SEM, and the machine was evacuated by the standard procedures. Imaging was done at an accelerating voltage of 15kV, and the working distance between the tip of the electron gun and samples was kept ten millimeters.

Thermogravimetric /Differential Thermal Analysis (TGA/DTA)

To study the thermal behavior and identification of the phase transformation temperature of the as prepared manganese oxide precursor particles, the latter were heated in the TGA/DTA analyzer (Diamond TGA/DTA Perkin Elmer) in the temperature range of $30\text{--}800\text{ }^\circ\text{C}$ in the flow of air at a heating rate of $5\text{ }^\circ\text{C min}^{-1}$.

Fourier Transform Spectrometry (FTIR)

Selected batches of the as-prepared and heat-treated powders were analyzed with Fourier Transform Infrared Spectrometer (Shimadzu, IRPrestige-21, FTIR-8400). In each case, the analyte was thoroughly mixed with KBr, transferred to the sample cup of the Diffuse Reflectance Accessory (DRS-8000A) and scanned from $4000\text{ to }400\text{ cm}^{-1}$.

X-ray Diffractometry (XRD)

In order to get a clue about the crystallinity of the desired batches of the as synthesized and heat-treated powders, they were analyzed by using X-ray diffractometer (JEOL JDX-3532). $\text{Cu K}\alpha$ radiations were used for the analysis in the 2θ range of $5\text{--}80^\circ$. The step angle and scan speed were respectively kept 0.01° and 0.1 s^{-1} during the scanning process. The obtained data were interpreted with the help of software, named as JDX-3500 and CMPR.

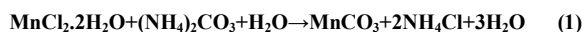
Point of Zero Charge (PZC)

Point of zero charge (PZC) of the desired sample was determined by using a well-established salt addition method [15].

For this purpose, 0.1g of manganese oxide powder was dispersed in 500 mL of 0.01 M NaNO₃ solution by sonicating the dispersion for two hours. Then a series of 100 mL reagent bottles were arranged, and to each bottle, 50 mL of the above dispersion was added. The next step was to adjust pH of these solutions in the respective bottles from 2-10. For this purpose, 0.1N HCl or NaOH solutions were used to set the required range of pH, and the pH was measured by a pH meter (NeoMet model number, pH-250L, Korea). The suspensions were agitated for a period of 24 h using water bath shaker (WSB-30 model). After aging, pH of each suspension was measured as pH_i (pH initial), and then 1g of NaNO₃ salt was added to each bottle. The suspensions were again agitated for 24 h in water bath shaker and pH of the dispersions was measured as pH_f (pH final). PZC was then estimated from the plot of ΔpH (pH_f - pH_i) versus pH_i.

Results and Discussion

Manganese oxide precursor was precipitated in the form of manganese carbonate, applying an aqueous solution of ammonium carbonate as the precipitant with manganese chloride solution. The precipitation reaction can be expressed as:



Reactant mixtures, comprising ammonium carbonate and manganese chloride were aged at room temperature in stoppered glass vessels under various conditions including stirring, sonication and under silent (without any external agitation) conditions for various periods of time. Each mixing resulted in precipitated solid. Scanning electron microscopic analysis of the obtained solids showed that particle's morphology and uniformity was a function of the experimental conditions, applied. Monodispersity in particle's morphology was achieved within limited compositions of the reactant mixtures and aging time. This revealed that the surplus ionic species affected the development of primary particles either by agglomeration or by the surface precipitation process.

Fig. 1 shows the SEM images of the particles obtained under conditions given in the caption. All the three images show that particles were of spherical morphology, having a size of about 2 μm. The existence of nanoparticles on each of the large particle suggested that second nucleation might have occurred; giving rise to

nanoparticles, which then got adhered to the larger particle by the process of homocoagulation.

The particles obtained under sonication as well as under silent conditions, i.e., Fig. 1A and 1C showed that under these conditions the obtained particles were not uniform and some sort of agglomeration was present. On the other hand, particles obtained under magnetic stirring (SEM, Fig. 1B) possessed a high degree of uniformity in shape and size. The presence of monodispersity made the particles given in Fig 1B as material for further characterization. Moreover, researchers have produced manganese carbonate in various morphologies by following some other types of experimental processes as well [12, 17]. It is mentioned that since particle's morphology play a vital role in all powder based hi-tech applications; therefore, we consider that the particles produced in this work may serve as excellent material to be used in processes like adsorption and catalysis.

Powder sample shown in Fig. 1B was analyzed with FTIR. The recorded spectrum (Fig. 2), composed of absorption bands at different positions, corresponding to different types of chemical groups on particle's surface as described below:

The obtained spectrum shows the existence of absorption bands at various frequencies that suggested the presence of different chemical groups in the tested material. A major band appeared at 3200-3600 cm⁻¹ corresponded to the stretching vibration of the water molecule [18]; a small dip at 1625-1637 cm⁻¹, corresponded to the bending vibration of H₂O molecule [19]. In the same way, the band located from 1800-400 cm⁻¹ stands for CO₃²⁻ anions. This peak suggests that the as prepared substance is carbonate of manganese (MnCO₃) [19]. A broad absorption peak at 1400-1500 cm⁻¹ and a narrow one at 1050 cm⁻¹ can be assigned to asymmetric stretching vibration mode of CO₃²⁻ anions while the bands at about 862 and 712 cm⁻¹ stand for the bending vibration of CO₃²⁻ anions [20]. There is also present a sharp peak at 2490 cm⁻¹, which can be ascribed to the adsorbed CO₂ [20]. The peak at 2489 cm⁻¹ confirmed the presence of carbonate anion. Also, a weaker band at 1798 cm⁻¹ was attributed to a combined band of Mn²⁺ and CO₃²⁻ [21]. In addition to these all, The existence of two sharp bands located at 725 and 860 cm⁻¹ along with a broad band in the range of 1400 cm⁻¹ were the characteristic bands of MnCO₃ [22]. Keeping in view the above findings, the particles presented in Fig. 1B may be titled as MnCO₃.

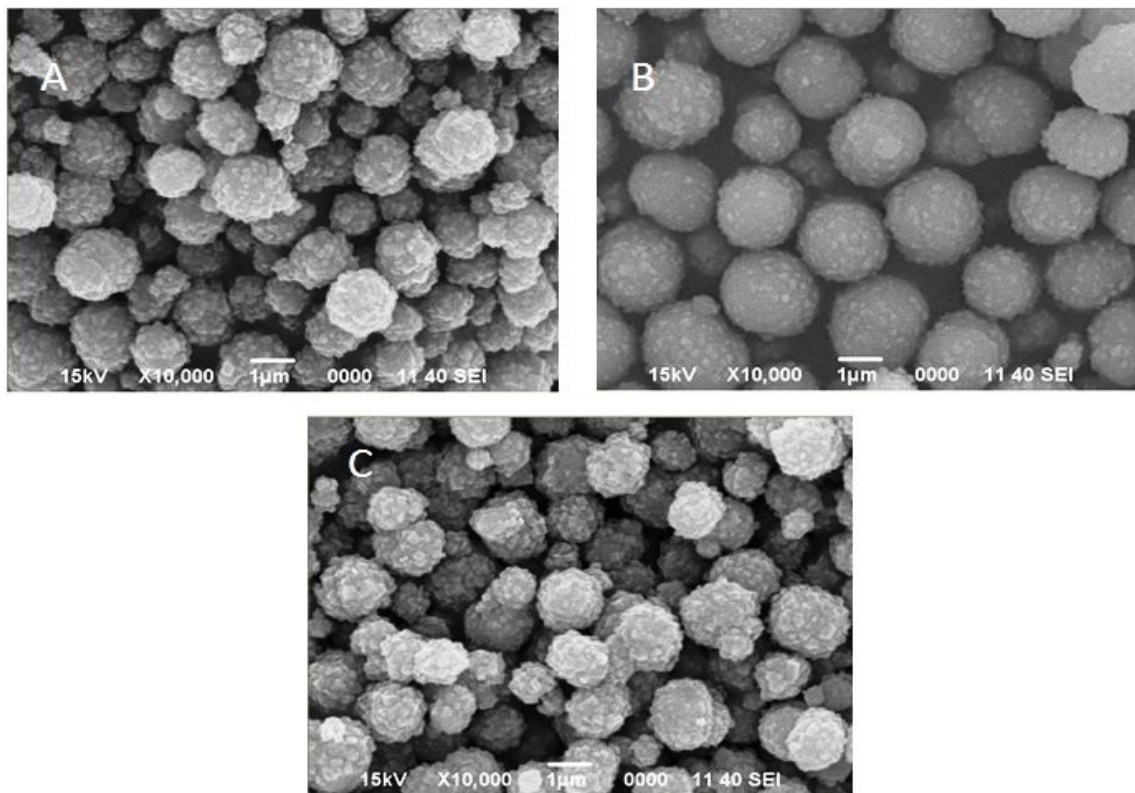


Fig. 1: Scanning Electron Micrograph (SEM) of the manganese oxide precursor particles (MnCO_3) obtained at room temperature by mixing of manganese chloride and ammonium carbonate in the molar ratio of 1 by sonication (A), stirring at room temperature (B) and under silent (without any external agitation) condition (c).

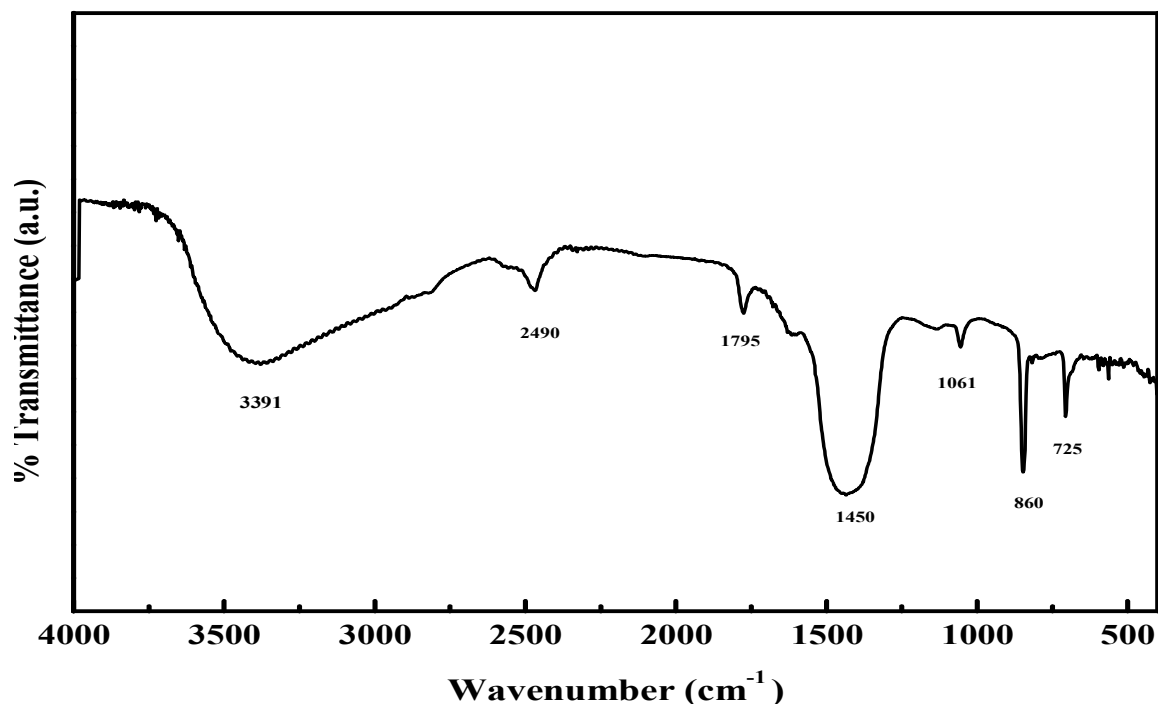


Fig. 2: Fourier Transform Infrared (FTIR) spectrum of the particles shown in Fig. 1(B).

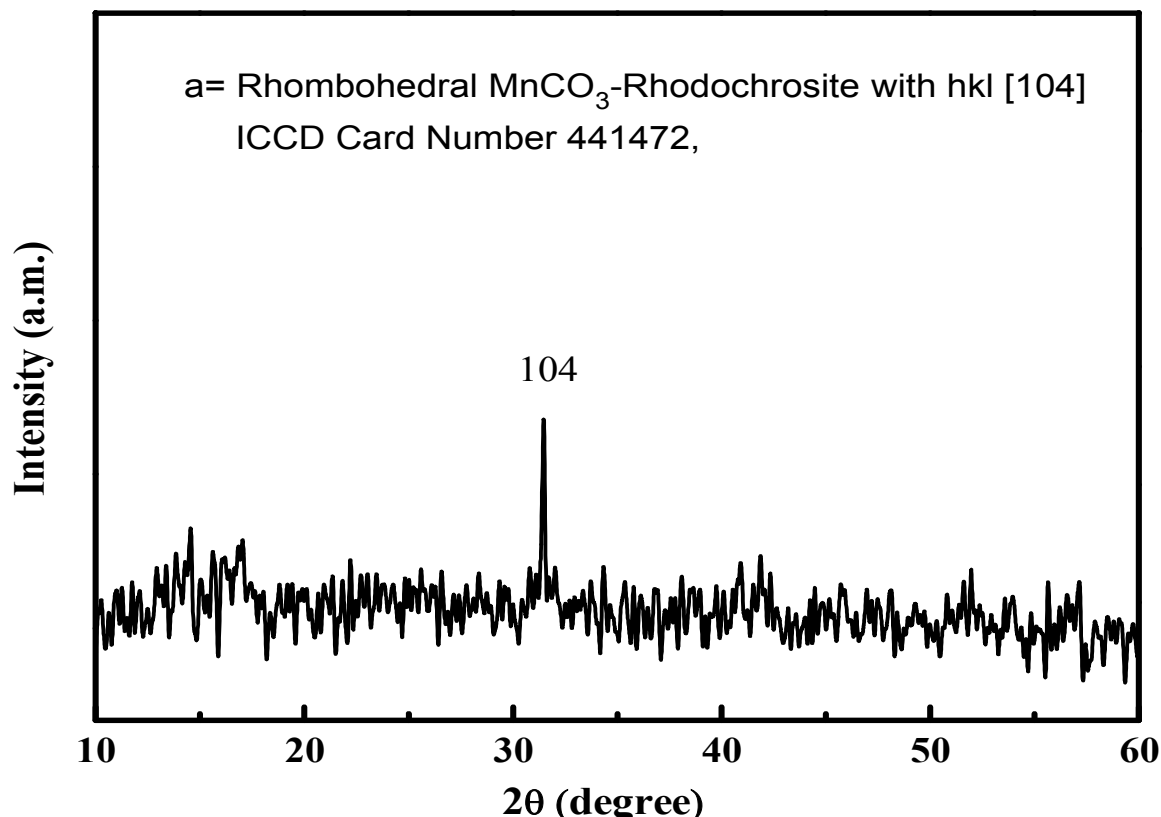


Fig. 3: X-ray diffraction (XRD) patterns of the particles shown in Fig. 1 (B).

The same particles (SEM, Fig.1B) were investigated with x-ray diffractometer. The obtained diffraction patterns (XRD, Fig. 3) showed that the test particles demonstrated some crystallinity [23, 24] and the observed peaks were characteristics of manganese carbonate, Rhodochrosite in Rhombohedral crystal system with JCPDS-ICDD 4401472. The crystallite size determined according to the Debye- Scherer equation (Eqn. 2) [25] was found to be 38.28 nm.

$$D = [(K\lambda) / \beta \cos \theta] \quad (2)$$

where,

D = Crystallite size

K =Shape factor (0.98)

λ = Wavelength of x. rays (1.54 Å)

β = Half angle of diffracted peak

θ = Angle of diffraction of x. rays

The presence of crystallinity in the particles showed that aggregation of the precursors of the full-grown particles occurred in a controlled manner under the given set of conditions and thus resulted in crystallinity in the end product. However, conflicting

results have been given in the literature regarding the bulk properties of manganese carbonate, prepared through different precipitation methods [13, 26]. Some researchers produced it in crystalline form while others reported it in amorphous form. As such, it may be established from the work performed in the current study as well as that reported in the literature that the bulk properties of the precipitated manganese carbonate can be tuned by proper optimization of the composition of the starting reactant mixtures and the applied precipitation conditions [27].

Thermal analysis of the selected batch (Fig. 1B) was carried out in a thermogravimetric analyzer in the temperature range of 30 to 800 °C. For this purpose, the sample was heated in the air atmosphere at the heating rate of 5 °C min⁻¹, and the obtained thermograms are shown in Fig. 4. Inspection of obtained thermograms showed two weight loss regions. The first weight loss occurred during heating the sample up to 150 °C while the second weight loss was obtained at a temperature ranging from 300 - 440 °C. Among the mentioned weight losses, the first one was smaller in magnitude while the second one was of high magnitude. Loss of water, adsorbed on the surface of the test material caused the first weight

loss whereas the second was caused by phase transformation from manganese carbonate to manganese oxide. In order to confirm the mentioned statement, we believe that the changes caused due to thermal treatment took place according to the reaction given in Eq.3, as there was a small difference between the theoretical weight loss (40.06 wt %), calculated from Eq.3 and the weight loss found practically (41.60 wt.%).

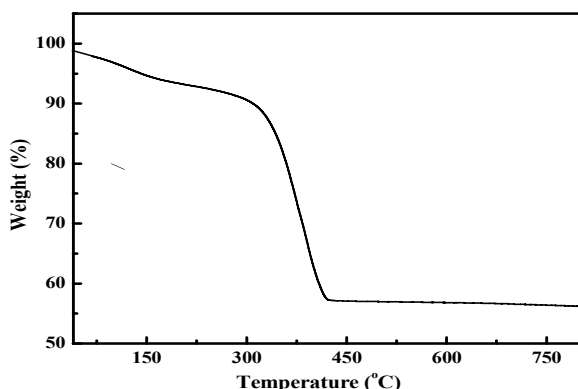
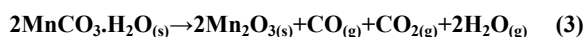


Fig. 4: Thermal analysis of the particles shown in Fig. 1B.

These findings also helped us to conclude that the material shown in Fig. 1B is hydrated manganese carbonate ($\text{MnCO}_3 \cdot \text{H}_2\text{O}$). Literature reveals that other peoples also have prepared manganese oxide from thermal treatment of manganese carbonate irrespective of the morphologies of the precursor (manganese carbonate) [13, 28].

By using the TGA data (Fig. 4), the activation energies associated with the observed weight losses were estimated using a well-known Coats Redfern equation (Eq. 4) [29]

$$\text{Ln}[-\text{Ln}(1-\alpha/T^2)] = -E_a/RT + \text{Ln}[(AR/\beta E)(1-(2RT/E))] \quad (4)$$

where,

- α = Frictional decomposed mass of the original material at time t,
- β = dT/dt (heating rate),
- $\text{Ln}[(AR/\beta E)(1-(2RT/E))] =$ approximately constant
- T = Absolute temperature,
- R = Universal gas constant

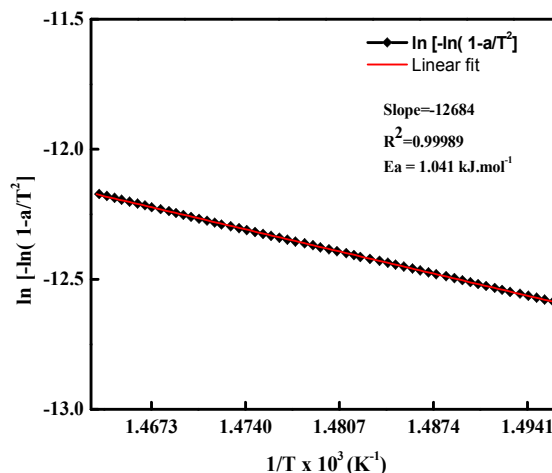


Fig. 5: $\ln[-\ln(1-\alpha/T^2)]$ vs $1/T \times 10^3 \text{ K}^{-1}$.

While α was calculated from the TGA data by using the following equation (Eqn. 5):

$$\alpha = (W_i - W_t) / (W_i - W_f) \quad (5)$$

By plotting the data in terms of $\ln[-\ln(1-\alpha/T^2)]$ against $1/T$ for the weight loss steps, 1.041 kJ/mol of activation energy was measured from the slope of the plot (Fig. 4). This energy can be attributed to the removal of physically adsorbed surface water molecules and phase transformation of the precursor MnCO_3 to Mn_2O_3 .

Heat Treatment

The thermal analysis of the particles given in Fig. 1 B, it was noticed that the tested material lost almost all of the thermally decomposable material beyond 600 °C and remained stable up to 750 °C. Thus in order to know the compositions of the heat treated products, more experiments were carried out in which rather larger amounts of the same materials were heated at different heating rates of 5, 10 and 15 °C min^{-1} up to 800 °C and hold them at the latter temperature for 1h. No sintering was found as a result of heating the material at different rates. In addition, the particles could be easily dispersed in an aqueous and ethanolic medium by the process of sonication. SEM analysis in Fig. 6 showed that calcination reduced the size of the particles shown in Fig. 1B and reduction in size was clearly due to loss of material during the calcination process. Other researchers have reported a similar trend of reduction in particle size of the MnCO_3 by the calcination process as well [18, 20].

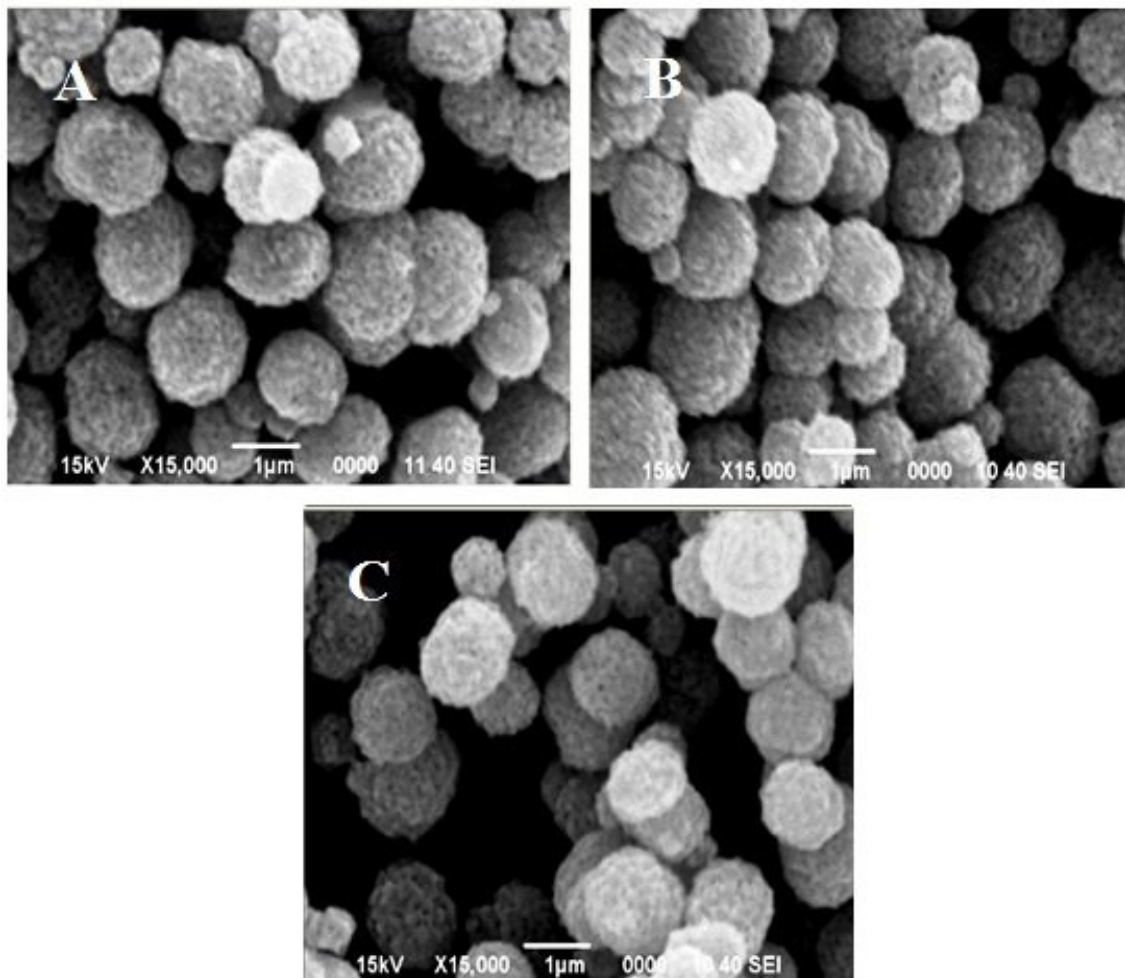


Fig. 6: Scanning Electron Micrographs (SEM) of particles given in Fig 1.B at different calcination rates of 5 °C/min (Fig. A), at 10 °C/min (Fig. B), and at 15 °C/min, (Fig C) up to 800 °C for one hour.

The scanning electron microscopy shows that spherical morphology of the precursor (MnCO_3), was retained by the resulted Mn_2O_3 particles and they kept their shape integrity to a maximum extent. Moreover, it was noted that the obtained Mn_2O_3 particles were porous with a rough surface. The weight loss due to removal of water and some other temperature nonresistant materials is also clear from the SEM image (SEM Fig. 6). The behavior of reduction in size and enhanced porosity with calcination of MnCO_3 has been reported elsewhere [30, 31]. Furthermore, calcinations of the test material disclosed that fabrication of a single particle was a result of homocoagulation of submicron sized primary particles that formed secondary agglomerates of MnCO_3 particles [32]. During calcinations at high temperature, the morphology of the as synthesized particles (Fig. 6) was found to be unaffected by the change in heating rate, and the spherical morphology was retained in all the three cases confirming the

stability of the obtained particles under the given set of experimental conditions.

X-ray diffractometric analysis (Fig. 7) of the particles shown in Fig. 1B, calcined at different rates (5, 10 and 15 °C / min) up to 800 °C, showed the production of Orthorhombic Mn_2O_3 (bixbyite) with hkl value (222). The calcined sample exhibited XRD peaks which revealed well-developed reflections of Mn_2O_3 (ICCD card number 240508), showing that the synthesized samples were pure Mn_2O_3 as no peak of any other phase was detected. This observation shows that the obtained end product at either of the mentioned heating rates, clearly supported the phase transition reaction, mentioned in equation 2. However, the variation in heating rates altered the peak intensities, and much intense peaks were obtained at elevated rates than those, obtained at lower rates [33]. This pointed to the fact that the thermal energy provided by the calcinations

controlled the crystalline phase and particle size [34]. The crystallite size was found to be 38.26 nm, 38.28 and 38.25 nm for the sample calcined at 5, 10 and 15° C per minute. The obtained results showed that crystallite was almost independent of the heating rates and illustrated nearly same value. Whereas the particle size roughly calculated from the magnification bar is nearly 1 μm , showing that the calcined sample is polycrystalline, i.e. composed of a large number of crystals of the same origin. Based on the XRD study, particles in Fig. 6C showed a high degree of crystallinity (XRD Fig. 7C), therefore, these particles were used for further characterizations.

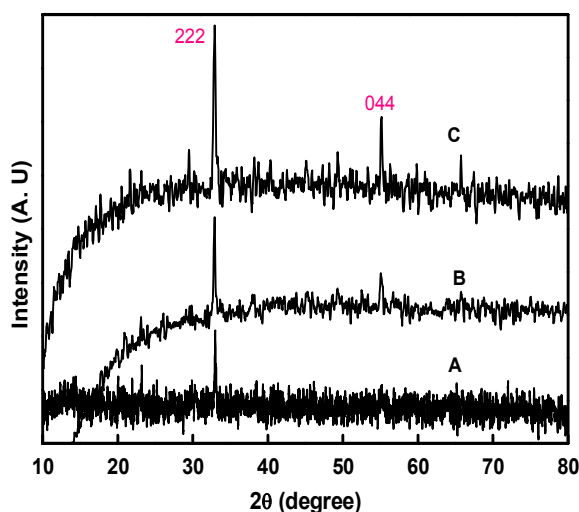


Fig. 7: X-ray diffractometric (XRD) patterns of particles given in Fig. 1B, calcined for one hour upto 800°C at the rate of 5 °C/min (A), 10 °C/min (B), and 15 °C/min (C).

Fourier transform infrared spectroscopy of the sample (SEM Fig. 6C) also confirmed the formation of Mn_2O_3 as a result of thermal treatment of the as prepared particles, MnCO_3 . The spectrum (FT-IR, Fig. 8) obtained for the calcined particles (SEM Fig. 6C) showed absorption bands at various positions that matched well with the spectrum, reported for manganese oxide elsewhere [35, 36]. These bands at 3450 cm^{-1} were due to the bending vibrations of a hydroxyl group of the adsorbed water [36]. The absorption bands attained at 670 and 573 cm^{-1} in fact referred to the asymmetric and symmetric stretching vibrations of Mn-O-Mn bond of Mn_2O_3 [13]. The band positioned in the range of 520 cm^{-1} could be ascribed to the bending vibration of Mn-O-Mn bond of Mn_2O_3 .

In order to have an idea about the surface charge and particles behavior towards different

electrolytes along with its susceptibility towards pH variation, the PZC of the end product (SEM, Fig. 6C) was estimated by the salt addition method. The results were plotted in Fig. 9 by plotting ΔpH ($\text{pH}_f - \text{pH}_i$) versus pH_i . Where, pH_i and pH_f correspond to pH of the dispersions of the manganese oxide powders before and after the addition of a large amount of sodium nitrate salt during the pH measurement process. The graph showed that the curve intersected the $\Delta\text{pH}=0$ at $\text{pH} \sim 6.00$. This pH value was chosen as the PZC, and it was a bit at a smaller pH side of the PZC values reported by other researchers [37, 38] obviously because of difference in composition of the electrolyte dispersions.

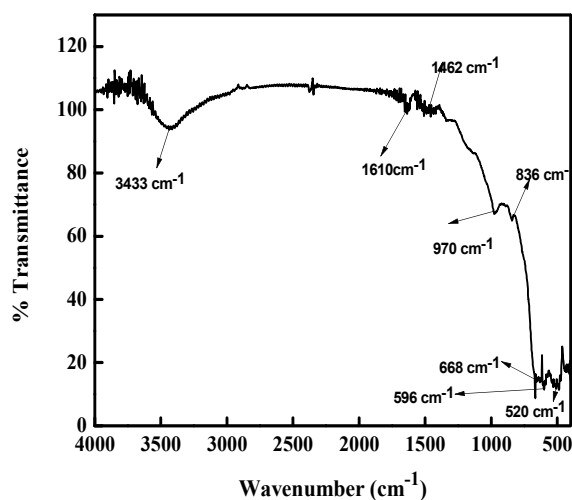


Fig. 8: Fourier Transform Infrared (FTIR) spectra of the particles in Fig. 6C.

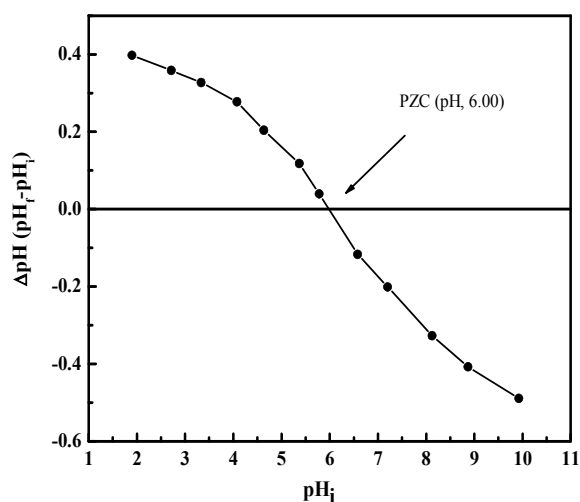


Fig. 9: Variation of ΔpH ($\text{pH}_f - \text{pH}_i$) as a function of pH_i of the particles shown in Fig. 6C.

Conclusions

- Uniform spherical particles of MnCO₃ were precipitated from aqueous solutions of manganese chloride with ammonium carbonate.
- Uniformity of the precipitated particles with respect to size and morphology was dependent upon the composition of the reactant mixture, agitation, and aging in a sensitive manner. Monodispersed particles were produced under a narrow set of the experimental conditions.
- Calcination at 800 °C transformed MnCO₃ to Mn₂O₃ particles, while particle shape integrity retained to a significant extent.
- The obtained particles were uniform in size, crystalline in nature and possessed high level purity as justified by XRD and FT-IR spectrum, showing characteristic peaks of desired products, i.e., MnCO₃ and Mn₂O₃ only.
- High temperature calcinations rate improved crystallinity of the synthesized Mn₂O₃ particles, while morphology and crystallite size remained unaffected.

Acknowledgments

The authors are thankful to the National Centre of Excellence in Physical Chemistry, University of Peshawar, Khyber Pakhtunkhwa, Pakistan and the Higher Education Commission of Pakistan for providing facilities and financial support for the present research work.

References

1. N. Talebian, S. M. Amininezhad and M. Doudi, Controllable synthesis of ZnO nanoparticles and their morphology-dependent antibacterial and optical properties. *J. Photoch. Photobio. B.*, **120**, 66 (2013).
2. S. M. Pourmortazavi, M. R. Nasrabadi, A. A. Davoudi-Dehaghani, A. Javidan, M.M. Zahedi and S. S. Hajimirsadeghi, Statistical optimization of experimental parameters for synthesis of manganese carbonate and manganese oxide nanoparticles. *Mater. Res. Bull.*, **47**, 1045 (2012).
3. Y. Dai, H. Jiang, Y. Hu and C. Li, Hydrothermal synthesis of hollow Mn₂O₃ nanocones as anode material for Li-ion batteries. *RSC. Adv.*, **3**, 19778 (2013).
4. D. M. Robinson, Y. B. Go, M. Mui, G. Gardner, Z. Zhang, D. Mastrogiovanni, E. Garfunkel, J. Li, M. Greenblatt and D. C. Dismukes, Photochemical water oxidation by crystalline polymorphs of manganese oxides: Structural requirements for catalysis. *J. Am. Chem. Soc.*, **135**, 3494 (2013).
5. C. Wang, L. Yin, L. Zhang, D. Xiang and R. Gao, Metal oxide gas sensors: sensitivity and influencing factors. *Sensors.*, **10**, 2088 (2010).
6. H. Z. Wang, H. L. Zhao, B. Liu, X. T. Zhang, Z. L. Du and W. S. Yang, Facile preparation of Mn₂O₃ nanowires by thermal decomposition of MnCO₃. *Chem Res Chinese U.*, **26**, 5 (2010).
7. H. Kurihara, T. Yajima and S. Suzuki, Preparation of cathode active material for rechargeable magnesium battery by atmospheric pressure microwave discharge using carbon felt pieces. *Chem. Lett.*, **37**, 376 (2008).
8. Y. Ueda, A. I. Kolesnikov and H. Koyanaka, Sensing hydrogen gas concentration using electrolyte made of proton conductive manganese dioxide. *Sensor. Actuat. B-Chem.*, **155**, 893 (2011).
9. X. Shen, Z. Ji, H. Miao, J. Yang and K. Chen, Hydrothermal synthesis of MnCO₃ nanorods and their thermal transformation into Mn₂O₃ and Mn₃O₄ nanorods with single crystalline structure. *J. Alloys Compd.*, **509**, 5672 (2011).
10. S. Devaraj and N. Munichandraiah, Effect of crystallographic structure of MnO₂ on its electrochemical capacitance properties. *J. Phy. Chem. C.*, **112**, 4406 (2008).
11. B. Li, G. Rong, Y. Xie, L. Huang, and C. Feng, Low-temperature synthesis of MnO₂ hollow urchins and their application in rechargeable Li⁺ batteries. *Inorg. Chem.*, **45**, 6404 (2006).
12. L. X. Yang, Y. J. Zhu, H. Tong and W. W. Wang, Submicrocubes and highly oriented assemblies of MnCO₃ synthesized by ultrasound agitation method and their thermal transformation to nanoporous Mn₂O₃. *Ultrason. Sonochem.*, **14**, 259 (2007).
13. H. Koyanaka, Y. Ueda, K. Takeuchi and A. I. Kolesnikov, Effect of crystal structure of manganese dioxide on response for electrolyte of a hydrogen sensor operative at room temperature. *Sensor. Actuat. B-Chem.*, **183**, 641 (2014).
14. I. U. Haq, K. Akhtar and Z. U. Khan, Characterization of monodispersed γ-Al₂O₃ particles, synthesized by homogeneous precipitation under reflux boiling. *High Temp. Mater. Proc.*, **34**, 325 (2015).
15. X. Duan, X. J. Lian, J. Ma, T. Kim, W. Zheng, Shape-controlled synthesis of metal carbonate nanostructure via ionic liquid-assisted hydrothermal route: the case of manganese carbonate. *Cryst. Growth. Des.*, **10**, 4449 (2010).
16. M. J. Aragon, C. P. Vicente and J. L. Tirado, Submicronic particles of manganese carbonate

- prepared in reverse micelles: A new electrode material for lithium-ion batteries. *Electrochem commun.*, **9**, 1744 (2007).
- H. Chen and J. He, Facile synthesis of monodisperse manganese oxide nanostructures and their application in water treatment. *J. Phys. Chem. C.*, **112**, 17540 (2008).
 - E. Nour, S. Teleb, N. A. Khsosy and M. Refat, A novel method for the synthesis of metal carbonates. I. synthesis and infrared spectrum of manganese carbonate, $\text{MnCO}_3 \cdot \text{H}_2\text{O}$, formed by the reaction of urea with manganese (II) salts. *Synth. React. Inorg. Met. Org. Chem.*, **27**, 505 (1997).
 - H. Cao, X. Wu, G. Wang, J. Yin, G. Yin, F. Zhang and J. Liu, Biomineralization strategy to $\alpha\text{-Mn}_2\text{O}_3$ hierarchical nanostructures. *J. Phys. Chem. C.*, **116**, 21109 (2012).
 - L. Liu, X. Zhang, R. Wang and J. Liu, Facile synthesis of Mn_2O_3 hollow and core-shell cube-like nanostructures and their catalytic properties. *Superlattices. Microstruct.*, **72**, 219 (2014).
 - L. Wang, F. Tang, K. Ozawa, Z. G. Chen, A. Mukherj, Y. Zhu, J. Zou, H. Cheng and G. Lu, A General Single-Source Route for the Preparation of Hollow Nanoporous Metal Oxide Structures. *Angew. Chem.*, **121**, 7182 (2009).
 - J. Xiao, P. Liu, Y. Liang, H. Li and G. Yang, High aspect ratio $\beta\text{-MnO}_2$ nanowires and sensor performance for explosive gases. *J. Appl. Phys.*, **114**, 073513 (2013).
 - X. Chu and H. Zhang, Catalytic decomposition of formaldehyde on nanometer manganese dioxide. *J. Mod. Appl. Sci.*, **3**, 177 (2009).
 - X. Zhang, L. Yue, D. Jin and Y. Zheng, A facile template-free preparation of porous manganese oxides by thermal decomposition method. *Inorg. Mat.*, **46**, 51 (2010).
 - K. Akhtar, M. Gul, I. U. Haq, R. A. Khan, A. Hussain, Synthesis and characterization of uniform fine particles of pure and chromium substituted manganese ferrite with low dielectric losses. *Ceram. Int.*, **42**, 18064 (2016).
 - V. Subramanian, H. Zhu, R. Vajtai, P. Ajayan and B. Wei, Hydrothermal synthesis and pseudocapacitance properties of MnO_2 nanostructures. *J. Phys. Chem. B.*, **109**, 20207 (2005).
 - H. Hu, J. -Y. Xu, H. Yang, J. Liang, S. Yang and H. Wu, Morphology-controlled hydrothermal synthesis of MnCO_3 hierarchical superstructures with Schiff base as stabilizer. *Mat. Res. Bull.*, **46**, 1908 (2011).
 - B. Parekh, P. Vyas, S. R. Vasant and M. Joshi, Thermal, FT-IR and dielectric studies of gel grown sodium oxalate single crystals. *Bull. Mater. Sci.*, **31**, 143 (2008).
 - J. Cao, Y. Zhu, Y. K. Bao, L. Shi, S. Liu and Y. Qian, Microscale Mn_2O_3 hollow structures: sphere, cube, ellipsoid, dumbbell, and their phenol adsorption properties. *J. Phys. Chem. C.*, **113**, 17755 (2009).
 - G. Zhu, D. Wang, W. Shan, Y. Tang and Y. Zhang, Facile fabrication of manganese carbonate and oxides shell structure. *J. Mater. Sci.*, **40**, 5025 (2005).
 - M. Zheng, H. Zhang, X. Gong, R. Xu, Y. Xiao, H. Dong, X. Liu and Y. Liu, A simple additive-free approach for the synthesis of uniform manganese monoxide nanorods with large specific surface area. *Nanoscale. Res. Lett.*, **8**, 1 (2013).
 - S. Mukherjee, A. K. Pal, S. Bhattacharya and J. Raittila, Magnetism of Mn_2O_3 nanocrystals dispersed in a silica matrix: Size effects and phase transformations. *Phys. Rev. B.*, **74**, 104413 (2006).
 - J. Regalbuto, Catalyst Preparation: Science and Engineering, page 256, CRC Press Tylor and Frances, p. 256 (2007).
 - Z. Chen, J. Lai and C. Shek, Influence of grain size on the vibrational properties in Mn_2O_3 nanocrystals. *J. Non-Cryst. Solids.*, **352**, 3285 (2006).
 - M. -S. Niasari, F. Mohandes, F. Davar and K. Saberyan, Fabrication of chain-like Mn_2O_3 nanostructures via thermal decomposition of manganese phthalate coordination polymers. *Appl. Surf. Sci.*, **256**, 1476 (2009).
 - X. Li, Y. Cui, X. Yang, W. -L. Dai and K. Fan, Highly efficient and stable $\text{Au/Mn}_2\text{O}_3$ catalyst for oxidative cyclization of 1, 4-butanediol to γ -butyrolactone. *Appl. Catal., B.*, **458**, 63 (2013).
 - M. Kosmulski, The pH-dependent surface charging and the points of zero charge. *J. Colloid interface. Sci.*, **253**, 77 (2002).
 - L. -C. Wang, Q. Liu, X. -S. Huang, Y. -M. Liu, Y. Cao and K. -N. Fan, Gold nanoparticles supported on manganese oxides for low-temperature CO oxidation. *Appl. Catal., B.*, **88**, 204 (2009).